

# A SURVEY FOR NEW STARS AND BROWN DWARFS IN THE OPHIUCHUS STAR-FORMING COMPLEX

T. L. ESPLIN<sup>1,2</sup> AND K. L. LUHMAN<sup>3,4</sup>

*Draft version May 21, 2020*

## ABSTRACT

We have performed a survey for new members of the Ophiuchus cloud complex using high-precision astrometry from the second data release of *Gaia*, proper motions measured with multi-epoch images from the *Spitzer Space Telescope*, and color-magnitude diagrams constructed with photometry from various sources. Through spectroscopy of candidates selected with those data, we have identified 155 new young stars. Based on available measurements of kinematics, we classify 102, 47, and six of those stars as members of Ophiuchus, Upper Sco, and other populations in Sco-Cen, respectively. We have also assessed the membership of all other stars in the vicinity of Ophiuchus that have spectroscopic evidence of youth from previous studies, arriving at a catalog of 373 adopted members of the cloud complex. For those adopted members, we have compiled mid-IR photometry from *Spitzer* and the *Wide-field Infrared Survey Explorer* and have used mid-IR colors to identify and classify circumstellar disks. We find that 210 of the members show evidence of disks, including 48 disks that are in advanced stages of evolution. Finally, we have estimated the relative median ages of the populations near the Ophiuchus clouds and the surrounding Upper Sco association using absolute  $K$ -band magnitudes ( $M_K$ ) based on *Gaia* parallaxes. If we adopt an age 10 Myr for Upper Sco, then the relative values of  $M_K$  imply median ages of  $\sim 2$  Myr for L1689 and embedded stars in L1688, 3–4 Myr for low-extinction stars near L1688, and  $\sim 6$  Myr for the group containing  $\rho$  Oph.

*Subject headings:* accretion, accretion disks - brown dwarfs - protoplanetary disks - stars: formation - stars: low-mass - stars: pre-main sequence

## 1. INTRODUCTION

The Ophiuchus complex of dark clouds is one of the nearest and most studied sites of active star formation ( $d \sim 140$  pc, Ortiz-León et al. 2017, 2018). It overlaps with the eastern edge of the Upper Scorpius subgroup (10 Myr; Picaud et al. 2012; Picaud & Mamajek 2016) in the Scorpius-Centaurus OB association and contains  $\sim 300$  known members (Wilking et al. 2008). Separate populations among those members exhibit ages ranging from  $\lesssim 1$  Myr for L1688 to several Myr for the group associated with the star  $\rho$  Oph (Greene & Meyer 1995; Luhman & Rieke 1999; Pillitteri et al. 2016). The current census of Ophiuchus members has resulted from surveys spanning more than 40 years, the first of which searched for stars with signatures of youth in the form of H $\alpha$ , X-ray, and mid-infrared (IR) emission (Wilking et al. 2008, references therein). Later surveys incorporated photometry and proper motions from optical and near-IR images (Luhman & Rieke 1999; Erickson et al. 2011), extending to progressively fainter magnitudes and lower masses (Alves de Oliveira et al. 2010, 2012; Geers et al. 2011; Mužić et al. 2012).

To work toward a more complete census of the stellar and substellar members of Ophiuchus, we have performed a new survey of the region that is based primarily on high-precision astrometry from the *Gaia* mission (Perryman et al. 2001; de Bruijne 2012) and proper motions

measured with multi-epoch imaging from the *Spitzer Space Telescope* (Werner et al. 2004). In this paper, we describe the current census of Ophiuchus (Section 2), our identification of candidate members via photometry, proper motions, and parallaxes (Section 3), and our spectroscopic classification of candidate members (Section 4). In addition, we determine whether the known members host circumstellar disks and classify the evolutionary stages of any detected disks (Section 5). Finally, we estimate the age differences among the populations projected against Ophiuchus (Section 6).

## 2. CATALOG OF KNOWN MEMBERS OF OPHIUCHUS

We have compiled all known objects with evidence of youth and measured spectral types within the boundary of Ophiuchus defined by Esplin et al. (2018), many of which are taken from previous catalogs of Ophiuchus members (Martín et al. 1998; Wilking et al. 2008; McClure et al. 2010; Erickson et al. 2011; Rigliaco et al. 2016). Luhman & Esplin (2020) constructed a similar catalog for an area outside of that boundary and within Upper Sco. The Ophiuchus boundary from Esplin et al. (2018) was defined to encompass a region in which the average offset from the median  $M_K$  of Upper Sco as a function of spectral type was significantly brighter, which is an indication of a younger average age. That region includes the three main dark clouds of Ophiuchus and a substantial area north of L1688, as shown in Figure 1.

Our sample of young stars toward Ophiuchus may contain both objects associated with the cloud complex and members of other populations in Sco-Cen, particularly Upper Sco. To help separate Ophiuchus members from other populations, we apply the kinematic criteria from Luhman & Esplin (2020) to data from the second data release (DR2) of the *Gaia* mission (Gaia Collaboration

<sup>1</sup> Steward Observatory, University of Arizona, Tucson, AZ, 85719, USA; taranesplin@email.arizona.edu

<sup>2</sup> Strittmatter Fellow

<sup>3</sup> Department of Astronomy and Astrophysics, The Pennsylvania State University, University Park, PA 16802; taran.esplin@psu.edu

<sup>4</sup> Center for Exoplanets and Habitable Worlds, The Pennsylvania State University, University Park, PA 16802.

et al. 2018). Luhman & Esplin (2020) used data from that survey to characterize the parallaxes and proper motion offsets ( $\Delta\mu_\alpha$ ,  $\Delta\mu_\delta$ ) for members of Ophiuchus, Upper Sco, and the remainder of the Sco-Cen complex. The proper motion offsets were defined as the difference between the observed proper motion and the motion expected at the star’s celestial coordinates and parallax if it had the median space velocity of members of Upper Sco ( $U, V, W = -5, -16, -7 \text{ km s}^{-1}$ ). Luhman & Esplin (2020) calculated density maps in  $(\pi, \Delta\mu_\alpha)$  and  $(\pi, \Delta\mu_\delta)$  for young stars projected against Ophiuchus. We have adopted thresholds for membership in Ophiuchus that approximate the 10% contours in those parameters. The resulting thresholds are shown in Figure 2. We adopt as members of Ophiuchus all known young stars that are within the boundary of Ophiuchus from Esplin et al. (2018), have *Gaia* parallaxes with errors of  $\leq 10\%$  and have  $1 \sigma$  errors in parallax and proper motion offsets that overlap with those criteria. We also assign membership to young stars outside of that spatial boundary that satisfy the kinematic criteria for Ophiuchus but no other population in Sco-Cen. Stars that lack precise parallaxes from *Gaia* are included in our membership catalog if they are within the Ophiuchus boundary, show spectroscopic evidence of youth, and do not have proper motion measurements that are inconsistent with membership. Due to the overlap in parallaxes and proper motions of members of Ophiuchus and other populations in Sco-Cen (Luhman & Esplin 2020), some of the stars in our catalog for Ophiuchus could be members of the latter.

SR 21 A and B,  $\rho$  Oph B, *Gaia* DR2 6049163679218606720 do not satisfy our proper motion criteria, but they are retained as members. The first two stars exhibit evidence of youth and significant reddening, indicating that they are associated with the Ophiuchus clouds.  $\rho$  Oph B and *Gaia* DR2 6049163679218606720 are likely companions to  $\rho$  Oph and GSS 37 given that they comprise pairs separated by only  $3''$  and  $1.1''$ , respectively.

We have adopted 373 young stars as members of Ophiuchus, 102 of which are newly classified in this work (Section 4). The catalog is presented in Table 1, which includes celestial coordinates, available measurements of spectral types, our adopted types, *Gaia* DR2 identification numbers, and the coordinate-based designations from the Point Source Catalog of the Two Micron All Sky Survey (2MASS; Skrutskie et al. 2006), the tenth data release of the United Kingdom Infrared Telescope Infrared Deep Sky Survey (UKIDSS, Lawrence et al. 2007), and the AllWISE Source Catalog from the *Wide-field Infrared Survey Explorer* (*WISE*; Wright et al. 2010). Table 1 also contains astrometry and optical photometry from *Gaia* DR2, near- and mid-IR photometry from various sources, disk classifications, and extinction estimates. One of the *Gaia* parameters is the renormalized unit weight error (RUWE, Lindegren 2018), which is an indicator of the quality of the astrometric fit.

In Table 1, we have assigned each adopted member of Ophiuchus to one of five groups based on their locations: objects projected against the dark clouds L1688, L1689, and L1709, objects in the vicinity of the star  $\rho$  Oph, and the remaining off-cloud stars. These assignments are also indicated in the map in Figure 1, where we have further

divided the L1688 population based on extinctions above and below  $A_J = 1.5$  ( $A_K = 0.57$ ) (Section 5.2). Using the available parallaxes with  $\sigma_\pi/\pi < 0.1$  from *Gaia* DR2 for our adopted members, we measure median distances of 138, 145, 137, and 140 pc for the groups toward L1688, L1689, L1709, and  $\rho$  Oph, respectively.

In Table 2, we present 59 young stars that have spectral classifications from previous studies or this work, are within the boundary of Ophiuchus complex, and exhibit kinematics inconsistent with membership in Ophiuchus. The catalog includes the available spectral classifications, photometry and astrometry from *Gaia* DR2, near-IR photometry from 2MASS, and flags indicating whether the *Gaia* astrometry is consistent with membership in Upper Sco or the remainder of Sco-Cen (Luhman & Esplin 2020).

### 3. IDENTIFICATION OF CANDIDATE MEMBERS

We have searched for new candidate members of Ophiuchus using parallaxes, proper motions, and optical and near-IR color-magnitude diagrams from several sources. In this section, we describe the procedures for the identification of those candidates.

#### 3.1. Proper Motions and Parallaxes from *Gaia* DR2

The high-precision astrometry from *Gaia* DR2 has greatly improved the ability to identify members of nearby associations (e.g., Gagné & Faherty 2018; Luhman 2018; Damiani et al. 2019; Herczeg et al. 2019). Among the 271 stars that we have adopted as previously known members of Ophiuchus, parallaxes with  $\leq 10\%$  errors are available from *Gaia* DR2 for 193 objects, which have spectral types as late as M8.0. We have searched for new members of Ophiuchus within our adopted boundary for the cloud complex by applying the kinematic criteria described in the previous section to astrometry from *Gaia* DR2. As done for a survey of Upper Sco by Luhman & Esplin (2020), we applied the criteria to *Gaia* sources with  $\pi/\sigma \geq 10$  and have ignored the *Gaia* astrometry if it is inconsistent with membership and may be unreliable based on a large value of RUWE ( $> 1.6$ ). These criteria produce 168 candidate Ophiuchus members that lack definitive assessments of youth from previous spectra.

Cánovas et al. (2019) recently identified 166 candidate members of Ophiuchus using astrometry from *Gaia* DR2. Among their candidates, 75 are also within our sample, four are slightly inconsistent with our proper motion criteria, and the remainder are either located outside of our adopted boundary for Ophiuchus or have previously reported spectral classifications.

#### 3.2. Proper Motions from the *Spitzer* Space Telescope

Because *Gaia* observes at optical wavelengths, it is not sensitive to Ophiuchus members that have high extinctions or very low masses. Detection of such objects requires IR data. Proper motions can be measured at IR wavelengths using the multiple epochs of imaging that are available for Ophiuchus from the Infrared Array Camera (IRAC; Fazio et al. 2004) on the *Spitzer* Space Telescope. From August 2003 to May 2009, IRAC operated with four broad-band filters centered at 3.6, 4.5, 5.8, and  $8.0 \mu\text{m}$  (denoted as [3.6], [4.5], [5.8], and [8.0]) and four  $256 \times 256$  arrays. The plate scale for each array was  $1''.2 \text{ pixel}^{-1}$ , corresponding to a field of view of

$5'2 \times 5'2$ . Point sources exhibited a FWHM of  $1''.6\text{--}1''.9$  for [3.6]–[8.0]. After the depletion of the cryogenics, IRAC continued to function with the [3.6] and [4.5] bands until January 2020.

We have retrieved all [3.6] and [4.5] images in the vicinity of Ophiuchus from the *Spitzer* archive. The Astronomical Observing Requests (AORs), program identifications (PIDs), and principal investigators (PIs) for those observations are listed in Table 3. The images within a given *Spitzer* observing window were combined, and they correspond to a single epoch in our analysis. The observations in each epoch spanned  $\lesssim 1$  month. These IRAC data have been used for studying outflows from young stars (Seale & Looney 2008), estimating star formation efficiencies and disk frequencies (Evans et al. 2009), searching for brown dwarfs with circumstellar disks (Harvey et al. 2010), confirming the nature of brown dwarfs selected by *WISE* (Griffith et al. 2012), measuring the variability of young stars (Günther et al. 2014), and constraining the properties of dust in molecular clouds (Lefèvre et al. 2014). In Figure 3, we show the fields that were observed in the six programs that covered the largest areas. Most of Ophiuchus was observed by programs 177 and 90071, which were separated by nine years. Those programs obtained two and nine 10.4 s exposures, respectively, at each position and filter.

We measured astrometry from the [3.6] and [4.5] images using the methods from Esplin et al. (2017). In summary, we performed the following steps for the final epoch of observations: 1) measured pixel coordinates, fluxes ( $F_\nu$ ), and signal-to-noise ratios (SNRs) for all sources in each image using the point-response-function fitting routine in the Astronomical Point Source Extractor (APEX, Makovoz & Marleau 2005); 2) applied the distortion correction from Esplin & Luhman (2016) to the pixel coordinates, 3) estimated the central coordinates and orientations of each image using astrometry from *Gaia* DR2, 4) iteratively refined those coordinates and orientations and 5) calculated celestial coordinates for each detection and averaged the detections from both bands of a single source. To avoid unreliable astrometry due to low SNR and saturation, we ignored sources with less than three total detections in a given epoch across the two bands and individual detections with  $F_\nu/(\text{exposure time}) > 0.73$  and  $> 0.82$  Jy/s in [3.6] and [4.5], respectively. For the other epochs, the central coordinates and orientations of images were aligned to the astrometry of the final epoch.

Proper motions were calculated for each source using a linear fit of the right ascension and declination as a function of time. In our analysis of proper motions, we ignored sources with errors in  $\mu_\alpha$  or  $\mu_\delta > 10$  mas yr $^{-1}$  and SNRs  $\leq 4.5$  and  $5.5$  in [3.6] and [4.5], respectively. These thresholds were determined in the manner described by Esplin et al. (2017). In Figure 4, we show the relative proper motions measured with IRAC for previously known members of Ophiuchus and new members from this work. The IRAC proper motions are included in Table 1.

To identify IRAC sources that have proper motions consistent with membership in Ophiuchus, we have applied thresholds that span the same ranges of values as the criteria used for *Gaia* DR2 and that are centered on the median IRAC motion of known members, as shown

in Figure 4. These criteria produce a sample of roughly 2000 candidates that are not previously known members. Most of the candidates are rejected via the photometric criteria described in the next section. Since the IRAC images extend beyond our adopted boundary for Ophiuchus (Figure 3), some of the proper motion candidates do so as well. Eight previously known members of Ophiuchus have IRAC proper motions that do not satisfy our criteria for membership. Seven of those stars exhibit enough extinction ( $A_V > 4$ ) and evidence of youth to indicate that they are associated with the Ophiuchus clouds, so we retain them as members. The one remaining object, 2MASS J16265128-2432419, has lower extinction, but its *Gaia* data are consistent with membership, so we adopt it as a member as well.

### 3.3. Color-magnitude Diagrams

To further refine the  $>2000$  Ophiuchus candidates selected with astrometry from *Gaia* and *Spitzer*, we have checked whether the candidates have positions in optical and near-IR color-magnitude diagrams (CMDs) that are similar to those of the previously known members of Ophiuchus.

We have searched for counterparts of the previously known members of Ophiuchus and the candidate members selected with *Gaia* and IRAC in publicly available photometric catalogs at optical and IR wavelengths. The data included in our analysis consist of:  $G$ ,  $G_{BP}$ ,  $G_{RP}$  (3300–10500, 3300–6800, 6300–10500 Å) from *Gaia* DR2;  $rizy_{P1}$  from the first data release of Pan-STARRS1 (PS1, Kaiser et al. 2002, 2010; Flewelling et al. 2016);  $ZYJHK$  from data release 10 of UKIDSS;  $JHK_s$  from the 2MASS Point Source Catalog; and  $JK_s$  from data release 6 of the VISTA Hemisphere Survey (VHS). We adopted the point-spread function (PSF) magnitudes from the stacked images in PS1 and the  $1''$  radius aperture magnitudes from UKIDSS and VHS. Potentially saturated measurements from these surveys were avoided in the manner described by Luhman et al. (2018).

In addition to public surveys, we have made use of photometry that we measured from the 3.6 and 4.5  $\mu\text{m}$  IRAC images and  $JHK_s$  images that we obtained with the Infrared Side Port Imager (ISPI) at the Cerro Tololo Inter-American Observatory (CTIO). We converted the 2013.4 epoch [3.6] and [4.5]  $F_\nu$  measurements from APEX into magnitudes using zero points selected to align with IRAC photometry from Luhman & Mamajek (2012). The ISPI images were obtained on the nights of April 28–30 in 2004. They cover a  $20' \times 20'$  field centered at  $(\alpha, \delta) = (246.542^\circ, -24.377^\circ)$  and have completeness limits near  $J = 18.5$ ,  $H = 17.7$ , and  $K_s = 16.7$ .

We combined and merged the above catalogs of photometry in the manner done for Upper Sco by Luhman et al. (2018). UKIDSS and VHS exhibit color-dependent offsets relative to 2MASS, so we have added 0.07,  $-0.04$ ,  $0.03$  mag to  $J$ ,  $H$ , and  $K$  from UKIDSS and 0.07,  $-0.03$  to  $J$  and  $K$  from VHS, which aligns those data to the 2MASS photometry for known M-type members of Upper Sco (Luhman & Esplin 2020). In our analysis, photometric measurements with errors greater than 0.1 mag are ignored. We have estimated the extinction for each source by dereddening it to the typical locus of young stars at the distance of Ophiuchus in  $H$  versus  $J - H$  (or  $K_s$  versus  $J - K_s$  when  $J - H$  was not available), as

done in our previous work (Esplin & Luhman 2017, references therein). These extinctions are used to deredden the photometry of the stars in our other CMDs, which helps to distinguish Ophiuchus members from field stars. In Section 5.2, we will compute separate extinctions for the adopted members in a way that utilizes their measured spectral types.

In Figure 5, we present extinction-corrected CMDs for previously known members of Ophiuchus and Upper Sco within Figure 3 and new members from this work. As done in our previous surveys (Luhman et al. 2018), each diagram has  $K_s$  on the vertical axis and a color between another band and  $K_s$  on the horizontal axis. In each CMD, we have defined a boundary that follows the lower envelope of known members. Among the candidates identified with *Gaia* and IRAC astrometry, 405 sources appear above a boundary in at least one CMD and do not fall below the boundaries of any CMDs, and thus are considered viable candidates.

## 4. SPECTROSCOPY OF CANDIDATE MEMBERS

### 4.1. Observations

We have obtained spectra of 148 candidate members of Ophiuchus from the previous section to confirm their membership via signatures of youth and to measure their spectral types. In addition, we have performed spectroscopy on 49 objects that were candidates early in our survey but that do not satisfy our latest criteria and we have observed 33 previously known members to improve their classifications, resulting in a total of 230 sources in our spectroscopic sample. There are 259 remaining candidates that lack either definitive assessments of youth from spectra or measured spectral types. Those objects are presented in Table 4. We note that more than a third of these candidates have been previously identified in the literature as potential or likely members of Ophiuchus. For instance, 2MASS 16244941-2459388 exhibits evidence of youth from previous spectroscopy (Rigliaco et al. 2016). Since it lacks a measured spectral type, we include it among the candidate members rather than the adopted members.

Optical spectroscopy was performed with the Cerro Tololo Ohio State Multi-Object Spectrograph (COSMOS) at the 4-m Blanco telescope at CTIO and the Inamori Magellan Areal Camera and Spectrograph (IMACS) on the Magellan I telescope at Las Campanas Observatory (Dressler et al. 2011). The former is based on an instrument described by Martini et al. (2011). Near-IR spectra were obtained with the Cornell Massachusetts Slit Spectrograph (CorMASS; Wilson et al. 2001) on the Magellan II telescope, the Astronomy Research using the Cornell Infra Red Imaging Spectrograph (ARCoIRIS) at the 4-m Blanco telescope at CTIO, FLAMINGOS-2 on the Gemini South Telescope (Eikenberry et al. 2004), and SpeX (Rayner et al. 2003) at the NASA Infrared Telescope Facility (IRTF). The instrument configurations are summarized in Table 5. The dates of the observations are listed in Table 6.

We reduced the optical spectra using routines in IRAF. The reduction steps included flat-field correction, spectral extraction, and wavelength calibration. The IR spectra from FLAMINGOS-2 and GNIRS were reduced in a similar manner with the addition of a step to correct

for telluric absorption using a spectrum of an A-type star that was observed at a similar airmass. Because the FLAMINGOS-2 spectra had low S/N, we binned the spectra by a factor of 15. The SpeX data were processed using the Spextool package (Cushing et al. 2004) and corrected for telluric absorption in the manner from (Vacca et al. 2003). The ARCoIRIS spectra were reduced with a modified version of Spextool. Examples of the optical and IR spectra are presented in Figures 6 and 7, respectively. The reduced spectra are provided in electronic files associated with those figures.

### 4.2. Spectral Classification

We have used our spectroscopic data to measure spectral types and check for signatures of youth that would support membership in Ophiuchus. The objects in our spectroscopic sample range from  $K_s \sim 9$ –17, which corresponds to spectral types of  $\sim$ M0 through early L for members of Ophiuchus. At those types, we can distinguish young objects from field stars via Li I absorption at 6707 Å and gravity-sensitive features such as Na I and the steam absorption bands (Martín et al. 1996; Luhman et al. 1997; Lucas et al. 2001). Spectral types were estimated for field stars using dwarf and giant spectral standards (Henry et al. 1994; Kirkpatrick et al. 1991, 1997; Cushing et al. 2005; Rayner et al. 2009). Optical spectral types of young objects were measured with averages of spectra of dwarf and giants standards (Luhman et al. 1997, 1998; Luhman 1999). IR spectra of young stars were classified using standard spectra constructed from optically-classified young objects (Luhman et al. 2017).

Our spectral classifications are presented in Table 6. We find that 159 of the objects in our spectroscopic sample that were not previously known members exhibit evidence of youth. We have classified the membership for those young stars in the following manner. Stars are adopted as members of Ophiuchus if they have 1) locations within the Ophiuchus boundary and *Gaia* parallaxes and proper motions consistent Ophiuchus (Luhman & Esplin 2020), 2) locations within Ophiuchus and no *Gaia* parallaxes or proper motions, or 3) locations outside of Ophiuchus and *Gaia* parallaxes and proper motions that are consistent with Ophiuchus and no other populations in Sco-Cen. If none of those sets of criteria are satisfied, then a young object is assigned to Upper Sco if 1) its *Gaia* parallaxes and proper motions are consistent with that population or 2) *Gaia* astrometry is not available and it is located outside of Ophiuchus. Stars that are not classified as members of Ophiuchus or Upper Sco and that have astrometry consistent with the remainder of Sco-Cen (Luhman & Esplin 2020) are assigned to that population. In that way, we classify 102, 47, and six of the young sources without previously reported spectral types as new members of Ophiuchus, Upper Sco, and the remainder of Sco-Cen, respectively. Five young stars have kinematics that are inconsistent with membership in any of the Sco-Cen populations. In Table 6, we indicate for each object whether it has evidence of youth and, if so, its assigned population. The spectral types of the new Ophiuchus members range from M1 to M9.5, including 23 with spectral types later than M6 ( $\lesssim 0.1 M_\odot$ ). Those objects also contain 6 of the 10 faintest known members of Ophiuchus in terms of extinction-corrected  $K_s$ .

## 5. CIRCUMSTELLAR DISKS IN OPHIUCHUS

We have compiled mid-IR photometry for our catalog of 373 adopted members of Ophiuchus from *WISE* and the *Spitzer Space Telescope* and have used those data to identify the presence of disks and to classify the detected disks.

### 5.1. Mid-IR photometry

*WISE* provides photometry in four bands centered at 3.4, 4.6, 12, and 22  $\mu\text{m}$  (*W1–W4*). For the members of Ophiuchus, we have adopted the measurements from the AllWISE Source Catalog when available. Among members of Ophiuchus that lack data in that catalog, five and two objects have counterparts in the *WISE* All-Sky Source Catalog and the AllWISE Reject Table, respectively. In total, *WISE* data are available for 349 members of Ophiuchus, which are included in Table 1. We visually examined the *WISE* images for each member to check for spurious detections, blending with nearby sources, and contamination from extended emission. We have flagged those data accordingly in Table 1. We found 99, 94, 67, and 41% of the members detected by *WISE* to have reliable photometry at *W1*, *W2*, *W3*, and *W4*, respectively.

We also have made use of photometry from *Spitzer* in the four bands of IRAC and the 24  $\mu\text{m}$  band ([24]) of the Multiband Imaging Photometer for *Spitzer* (MIPS; Rieke et al. 2004). The latter produced images with a field of view of  $5'.4 \times 5'.4$ . Point sources in those exhibits exhibited a FWHM of  $5''.9$ . When available, we have adopted flux measurements from the *Spitzer* Enhanced Imaging Products (SEIP) Source List. Those data were converted to magnitudes using zero points from Esplin et al. (2018), which were selected to match photometry from Luhman & Mamajek (2012) for Upper Sco. We inspected the SEIP mosaics to check for Ophiuchus members that were detected even though they lacked counterparts in the SEIP Source List and to check for blends with neighboring stars. For some of the latter cases, we performed PSF subtraction on the contaminating objects and manually measured photometry for the targets of interest. Aperture photometry for all detected objects without SEIP measurements was measured using routines in the IDL’s Astronomy Users Library. We present *Spitzer* photometry for 360 members of Ophiuchus in Table 1. We have flagged the measurements that may be uncertain due to blending with neighboring stars or bright extended emission.

### 5.2. Extinction Estimates

We wish to determine whether each member of Ophiuchus exhibits mid-IR excess emission from a circumstellar disk. Such excess emission can be detected by comparing colors between near- and mid-IR bands to those expected from stellar photospheres. However, because many members of Ophiuchus are embedded in dark clouds, their colors are subject to significant reddening from dust along the line of sight. As a result, we must apply a correction for that reddening in order to assess the presence of disk emission. We have estimated extinction in the  $K_s$  band ( $A_K$ ) for members of Ophiuchus based on the slope of near-IR spectra relative to the young spectroscopic standards from Luhman et al. (2017) when such data are available. Otherwise, we have derived extinc-

tions from color excesses in  $J - H$  (or  $H - K$  when  $J$  is unavailable) relative to the intrinsic values for young stars (Luhman & Esplin 2020) using the extinction law of Schlafly et al. (2016). The resulting estimates of  $A_K$  are included in Table 1.

### 5.3. Measurements of Excess Emission

We have used extinction-corrected mid-IR colors to identify excess emission from disks among the adopted members of Ophiuchus. In Figure 8, we have plotted the colors between  $K_s$  and six bands from *WISE* and *Spitzer* as a function of spectral type. The colors have been corrected for extinction using the values of  $A_K$  from Table 1 and the extinction relations from Indebetouw et al. (2005) and Schlafly et al. (2016). In each color, stars that lack disks form a blue sequence, corresponding to the intrinsic photospheric colors, although the sequence is not well-populated in  $K_s - W4$ . We have marked the thresholds for identifying excess emission from Esplin et al. (2018), which have been slightly shifted to reflect new estimates of the intrinsic photospheric colors of young stars (Luhman & Esplin 2020). We provide flags in Table 1 indicating whether an object has excess emission in each of the six mid-IR bands in Figure 8. Sources with no apparent excess emission at the longest available wavelength were labeled as likely having no excess at all wavelengths. Excesses that are only slightly above our thresholds in *W3*, *W4*, [8.0], and [24] are considered to be tentative. Although the B9 star V2394 Oph shows excess emission in the mid-IR bands relative to  $K_s$ , excesses are not present relative to *W1* or [3.6], so we classify it as having no excesses.

### 5.4. Disk Classifications

For the 210 sources with excess emission in at least one band, we have classified the evolutionary stages of the circumstellar disks using the methods that we have employed in Upper Sco (Luhman & Mamajek 2012; Esplin et al. 2018). We have considered the following disk classes (Kenyon & Bromley 2005; Rieke et al. 2005; Hernández et al. 2007; Luhman et al. 2010; Espaillat et al. 2012): *full* (optically thick with no large holes), *transitional* (optically thick with a large hole), *evolved* (optically thin with no large hole), *evolved transitional* (optically thin with a large hole), and *debris disk* (second generational dust from planetesimal collisions). We have assigned these classes based on extinction-corrected color excesses (Esplin et al. 2014, 2018), as shown in Figure 9. The resulting classifications are listed in Table 1. We classify 153, 7, 20, and 4 disks as full, transitional, evolved, and evolved or transitional, respectively. Because debris and evolved transitional disks are indistinguishable with mid-IR photometry, we have reported those classes as a single category, which contains 17 members.

## 6. RELATIVE AGES OF POPULATIONS IN OPHIUCHUS

Previous studies have reported evidence for multiple episodes of star formation within the Ophiuchus complex. For instance, Wilking et al. (2005) identified a population of low-extinction stars toward L1688 and found that they were older than the embedded population and roughly coeval with Upper Sco. As a result, they proposed that the same event triggered the formation of the

low-extinction stars near L1688 and the members of Upper Sco. Similarly, Pillitteri et al. (2016) found a group of stars surrounding the star  $\rho$  Oph that appeared to be older than the embedded stars in L1688 and possibly coeval with Upper Sco.

We can place new constraints on the relative ages of the populations in Ophiuchus by using *Gaia* parallaxes to estimate absolute magnitudes for the stars in our new census of Ophiuchus. Evolutionary models predict that low-mass stars evolve mostly vertically in the Hertzsprung-Russell during the first  $\sim 10$  Myr after they are born (e.g. Baraffe et al. 1998). As a result, relative values of extinction-corrected absolute magnitudes ( $M_K$ ) at a given spectral type can serve as proxies for relative ages. We have computed the  $M_K$  offsets of members of Ophiuchus from the median sequence for Upper Sco (Luhman & Esplin 2020) for spectral types of K5–M5, which spans a range of temperatures in which stars are expected to experience roughly the same evolution of luminosity with age for 1–10 Myr (Baraffe et al. 1998). Only objects with  $\sigma_\pi/\pi \leq 0.1$  from *Gaia* DR2 have been used in these calculations.

In Figure 10, we present a box-and-whisker plot of the  $M_K$  offsets for the populations of Ophiuchus described in Section 2 and shown on the map in Figure 1. For comparison, we have included data for known members of Upper Sco. Only the inner quartile ranges are plotted. We have estimated the errors of the median of each population via bootstrapping. Because a few of the groups have only a small number of known members, those errors can be quite large (e.g., the error of L1709 exceeds the inner quartile range). Along the top axis of Figure 1, we have indicated the ages that correspond to  $\Delta M_K$  assuming an age of 10 Myr for Upper Sco (Pecaut & Mamajek 2016) and the evolution of luminosity with age predicted by evolutionary models (Baraffe et al. 2015; Choi et al. 2016; Dotter 2016). The predicted changes in luminosity with age are similar between the non-magnetic and magnetic models for the ranges of temperature and ages in question (Feiden 2016). According to the data in Figure 10, the group in L1689 and the embedded stars in L1688 have similar median ages ( $\sim 2$  Myr) and are the youngest of the samples in Ophiuchus. L1709 is roughly coeval with those two populations given the errors. The measurements of  $\Delta M_K$  imply progressively older ages for the low-extinction stars in L1688 (3–4 Myr), the off-cloud stars ( $\sim 5$  Myr), and  $\rho$  Oph ( $\sim 6$  Myr), none of which are as old as Upper Sco. These results support the conclusion from Pillitteri et al. (2016) that the  $\rho$  Oph cluster is older than the embedded population in L1688. However, unlike that study, we find that the former is younger than Upper Sco. Given that the low-extinction stars toward L1688 and the off-cloud stars differ only slightly in age, have similar surface densities on the sky, and have indistinguishable kinematics and extinctions, we propose that they are members of the same population. The small age difference between those two samples could be explained by contamination of the low-extinction stars in front of L1688 by stars associated with the younger embedded population that have unusually low extinctions.

## 7. CONCLUSION

We have performed a survey for young stars associated with the Ophiuchus complex of dark clouds using proper

motions and parallaxes from *Gaia* DR2, proper motions measured with IRAC on *Spitzer*, and CMDs constructed with optical and IR photometry from various sources. We have obtained optical and near-IR spectra of candidates identified with those data to measure their spectral types and verify their youth, 159 of which are classified as new young objects. Based on available measurements of kinematics, most notably from *Gaia* DR2, we adopt 102, 47, and 6 of those sources as members of Ophiuchus, Upper Sco, and other populations in Sco-Cen, respectively. Using those same criteria, we also have assessed the membership of all other known young stars near Ophiuchus, arriving at a catalog of 373 adopted members of the cloud complex. The new Ophiuchus members have spectral types as late as M9.5 and include 6 of the 10 faintest known members in terms of extinction-corrected  $K_s$ . There remain 259 candidate members of Ophiuchus from this work that lack sufficient spectroscopic data to assess whether they are young.

We have compiled mid-IR photometry from *WISE* and *Spitzer* for the adopted members of Ophiuchus and have used those data to check for excess emission from circumstellar disks and to classify the evolutionary stages of the detected disks. We find that 210 of the members show evidence of disks, including 48 disks that are in advanced stages of evolution. In addition, we have estimated the relative median ages of the populations in Ophiuchus using offsets in  $M_K$  from the median sequence of Upper Sco for members with *Gaia* parallaxes and spectral types of K5–M5. Those offsets combined with the predicted evolution of luminosity with age Baraffe et al. (2015); Choi et al. (2016); Dotter (2016) imply median ages of  $\sim 2$  Myr for L1689 and embedded stars in L1688, 3–4 Myr for low-extinction stars near L1688, and  $\sim 6$  Myr for the group containing  $\rho$  Oph if we assume an age of 10 Myr for Upper Sco (Pecaut & Mamajek 2016). We suggest that most of the low-extinction stars toward L1688 may be members of a more widely distributed population that extends a few degrees to the north and west of that cloud.

We thank K. Allers for providing the modified version of Spextool for use with ARCoIRIS data. K. L. acknowledges support from NSF grant AST-1208239 and NASA grant 80NSSC18K0444. The *Spitzer Space Telescope* and the IPAC Infrared Science Archive (IRSA) are operated by JPL and Caltech under contract with NASA. *WISE* and *NEOWISE* are joint projects of the University of California, Los Angeles, and the Jet Propulsion Laboratory (JPL)/California Institute of Technology (Caltech), funded by NASA. 2MASS is a joint project of the University of Massachusetts and the Infrared Processing and Analysis Center (IPAC) at Caltech, funded by NASA and the NSF. The IRTF is operated by the University of Hawaii under contract NNH14CK55B with NASA. This work has made use of data from the European Space Agency (ESA) mission *Gaia* (<https://www.cosmos.esa.int/gaia>), processed by the *Gaia* Data Processing and Analysis Consortium (DPAC, <https://www.cosmos.esa.int/web/gaia/dpac/consortium>). Funding for the DPAC has been provided by national institutions, in particular the institutions participating in the *Gaia* Multilateral Agreement. The Center for Exoplanets and Habitable Worlds is supported by the Pennsylvania

State University, the Eberly College of Science, and the Pennsylvania Space Grant Consortium. Based in part on observations at Cerro Tololo Inter-American Observatory, National Optical Astronomy Observatory (NOAO Prop. ID: 2016A-0157 & 2017A-0103 and PI: T. Esplin), which is operated by the Association of Universities for Research in Astronomy (AURA) under a cooperative agreement with the National Science Foundation. Based on observations obtained at the Gemini Observatory (NOAO Prop. ID: 2016A-0139 and PI: T. Esplin), which is operated by the Association of Universities for Research in Astronomy, Inc., under a cooperative agree-

ment with the NSF on behalf of the Gemini partnership: the National Science Foundation (United States), the National Research Council (Canada), CONICYT (Chile), Ministerio de Ciencia, Tecnología e Innovación Productiva (Argentina), and Ministério da Ciência, Tecnologia e Inovação (Brazil). Based on observations obtained as part of the VISTA Hemisphere Survey, ESO Program, 179.A-2010 (PI: McMahon).

*Facilities:* Blanco (COSMOS, ARCoIRIS), Gemini:South (Flamingos-2), Gemini:North (GNIRS), IRTF (SpeX), *Spitzer* (IRAC, MIPS), *WISE*, *Gaia*, Magellan:Baade (IMACS).

## REFERENCES

- Allers, K. N., Jaffe, D. T., Luhman, K. L., et al. 2007, *ApJ*, 657, 511
- Alves de Oliveira, C., Moraux, E., Bouvier, J., & Bouy, H. 2012, *A&A*, 539, 151
- Alves de Oliveira, C., Moraux, E., Bouvier, J., et al. 2010, *A&A*, 515, 75
- Ansdell, M., Gaidos, E., Rappaport, S. A., et al. 2016, *ApJ*, 816, 69
- Baraffe, I., Chabrier, G., Allard, F., & Hauschildt, P. H. 1998, *A&A*, 337, 403
- Baraffe, I., Horneier, D., Allard, F., & Chabrier, G. 2015, *A&A*, 577, 42
- Bontemps, S., André, P., Kaas, A. A., et al. 2001, *A&A*, 372, 173
- Bouvier, J. & Appenzeller, I. 1992, *A&AS*, 92, 481
- Bowler, B. P., Liu, M. C., Kraus, A. L., & Mann, A. W. 2014, *ApJ*, 784, 65
- Cánovas, H., Cantero, C., Cieza, L., et al. 2019, *A&A*, 626, 80
- Casaanova, S., Montmerle, T., Feigelson, E. D., & Andre, P. 1995, *ApJ*, 439, 752
- Choi, J., Dotter, A., Conroy, C., et al. 2016, *ApJ*, 823, 102
- Cieza, L. A., Schreiber, M. R., Romero, G. A., et al. 2010, *ApJ*, 712, 925
- Cody, A. M., Hillenbrand, L. A., David, T. J., et al. 2017, *ApJ*, 836, 41
- Cohen, M. & Kuhl, L. V. 1979, *ApJS*, 41, 743
- Comerón, F., Testi, L., & Natta, A. 2010, *A&A*, 522, 47
- Cushing, M. C., Rayner, J. T., & Vacca, W. D. 2005, *ApJ*, 623, 1115
- Cushing, M. C., Tokunaga, A. T., & Kobayashi, N. 2000, *AJ*, 119, 3019
- Cushing, M. C., Vacca, W. D., & Rayner, J. T. 2004, *PASP*, 116, 362
- Damiani, F., Prisinzano, L., Pillitteri, I., Micela, G., & Sciortino, S. 2019, *A&A*, 623, 112
- de Bruijne, J. H. J. 2012, *Ap&SS*, 341, 31
- Dolidze, M. V. & Arakelian, M. A. 1959, *Astron. Zh.*, 36, 444
- Dotter, A. 2016, *ApJS*, 222, 8
- Dressler, A., Bigelow, B., Hare, T., et al. 2011, *PASP*, 123, 288
- Eikenberry, S., Albert, L., Forveille, T., et al. 2004, *Proc. SPIE*, 5492, 1196
- Elias, J. H. 1978, *ApJ*, 224, 453
- Erickson, K. L., Wilking, B. A., Meyer, M. R., Robinson, J. G., & Stephenson, L. N. 2011, *AJ*, 142, 140
- Españolat, C., Ingleby, L., Hernandez, J., et al. 2012, *ApJ*, 747, 103
- Esplin, T. L. & Luhman, K. L. 2016, *AJ*, 151, 9
- Esplin, T. L. & Luhman, K. L. 2017, *AJ*, 154, 134
- Esplin, T. L., Luhman, K. L., Faherty, J. K., Mamajek, E. E. & Bochanski, J. J. 2017, *AJ*, 154, 46
- Esplin, T. L., Luhman, K. L., & Mamajek, E. E. 2014, *ApJ*, 784, 126
- Esplin, T. L., Luhman, K. L., & Miller, E. B. 2018, *AJ*, 156, 75
- Evans, N. J., Dunham, M. M., Jørgensen, J. K., et al. 2009, *ApJS*, 181, 321
- Fazio, G. G., Hora, J. L., Allen, L. E., et al. 2004, *ApJS*, 154, 10
- Feiden, G. A. 2016, *A&A*, 593, A99
- Flewelling, H. A., Magnier, E. A., Chambers, K. C., et al. 2016, *arXiv:1612.05243*
- Gagné, J., & Faherty, J. K. 2018, *ApJ*, 862, 138
- Gaia* Collaboration, Brown, A. G. A., Vallenari, A., et al. 2018, *A&A*, 616, A1
- Gatti, T., Testi, L., Natta, A., Randich, S., & Muzerolle, J. 2006, *A&A*, 460, 547
- Garrison, R. F. 1967, *ApJ*, 147, 1003
- Geers, V., Scholz, A., Jayawardhana, R., et al. 2011, *ApJ*, 726, 23
- Geers, V. C., Van Dishoeck, E. F., Visser, R., et al. 2007, *A&A*, 476, 279
- Grasdalen, G. L., Strom, K. M., & Strom, S. E. 1973, *ApJ*, 184, 53
- Greene, T. P. & Meyer, M. R. 1995, *ApJ*, 450, 233
- Greene, T. P. & Young, E. T. 1992, *ApJ*, 395, 516
- Griffith, R. L., Kirkpatrick, J. D., Eisenhardt, P. R. M., et al. 2012, *AJ*, 144, 148
- Grosso, N., Montmerle, T., Bontemps, S., et al. 2000, *A&A*, 359, 113
- Gully-Santiago, M. A., Allers, K. N., & Jaffe, D. T. 2012, in *Proc. ASP Conf. Ser. Vol. 448, Cambridge Workshop on Cool Stars, Stellar Systems, and the Sun*, ed. C. M. Johns-Krull, M. K. Browning, & A. A. West (San Francisco, CA: ASP), 633
- Günther, H. M., Cody, A. M., Covey, K. R., et al. 2014, *AJ*, 148, 122
- Harvey, P. M., Jaffe, D. T., Allers, K. & Liu, M. 2010, *ApJ*, 720, 1374
- Henry, T. J., Kirkpatrick, J. D., & Simons, D. A. 1994, *AJ*, 108, 1437
- Herbig, G. H., & Bell, K. R. 1988, *Third Catalog of Emission-Line Stars of the Orion Population*, Vol. 3 (Santa Cruz, CA: Lick Observatory)
- Herczeg, G. J. & Hillenbrand, L. A. 2014, *ApJ*, 786, 97
- Herczeg, G. J., Kuhn, M. A., Zhou, X. et al. 2019, *ApJ*, 878, 111
- Hernández, J., Calvet, N., Hartmann, L., et al. 2005, *AJ*, 129, 856
- Hernández, J., Hartmann, L., Megeath, T., et al. 2007, *ApJ*, 662, 1067
- Houk, N., & Smith-Moore, M. 1988, *Michigan Catalogue of Two-dimensional Spectral Types for the HD Stars*. Vol. 4, (Ann Arbor: Univ. Mich.)
- Indebetouw, R., Mathis, J. S., Babler, B. L., et al. 2005, *ApJ*, 619, 931
- Kaiser, N., Aussel, H., Burke, B. E., et al. 2002, *Proc. SPIE*, 4836, 154
- Kaiser, N., Burgett, W., Chambers, K., et al. 2010, *Proc. SPIE*, 7733, 77330E
- Kamata, Y., Koyama, K., Tsuboi, Y., & Yamauchi, S. 1997, *PASJ*, 49, 461
- Kenyon, S. J., & Bromley, B. C. 2005, *AJ*, 130, 269
- Kirkpatrick, J. D., Henry, T. J., & Irwin, M. J. 1997, *AJ*, 113, 1421
- Kirkpatrick, J. D., Henry, T. J., & McCarthy, D. W. 1991, *ApJS*, 77, 417
- Kraus, A. L., Ireland, M. J., Cieza, L. A., et al. 2014, *ApJ*, 781, 20
- Lawrence, A., Warren, S. J., Almaini, O., et al. 2007, *MNRAS*, 379, 1599
- Lefèvre, C., Pagani, L., Juvela, M., et al. 2014, *A&A*, 572, 20
- Leous, J. A., Feigelson, E. D., Andre, P., & Montmerle, T. 1991, *ApJ*, 379, 683
- Lindgren, L. 2018, *Re-normalising the astrometric chi-square in Gaia DR2*, GAIA-C3-TN-LU-LL-124-01, <http://www.rssd.esa.int/doc.fetch.php?id=3757412>
- Lucas, P. W., Roche, P. F., Allard, F., & Hauschildt, P. H. 2001, *MNRAS*, 326, 695
- Luhman, K. L. 1999, *ApJ*, 525, 466

- Luhman, K. L. 2018, *AJ*, 156, 271
- Luhman, K. L., Allen, P. R., Espaillat, C., Hartmann, L., & Calvet, N. 2010, *ApJS*, 186, 111
- Luhman, K. L. & Esplin, T. L. 2020, *AAS Journals*, submitted
- Luhman, K. L., Herrmann, K. A., Mamajek, E. E., Esplin, T. L., & Pecaut, M. J. 2018, *AJ*, 156, 76
- Luhman, K. L., Liebert, J. & Rieke, G. H. 1997, *ApJ*, 489, 165
- Luhman, K. L., & Mamajek, E. E. 2012, *ApJ*, 758, 31
- Luhman, K. L., Mamajek, E. E., Shukla, S. J., & Loutrel, N. P. 2017, *AJ*, 153, 46
- Luhman, K. L. & Rieke, G. H. 1999, *apj*, 525, 440
- Luhman, K. L., Rieke, G. H., Lada, C. J., & Lada, E. A. 1998, *ApJ*, 508, 347
- Maheswar, G., Manoj, P., & Bhatt, H. C. 2003, *A&A*, 402, 963
- Makovoz, D. & Marleau, F. R. 2005, *PASP*, 117, 1113
- Manara, C. F., Testi, L., Natta, A., & Alcalá, J. M. 2015, *A&A*, 579, 66
- Martín, E. L., Montmerle, T., Gregorio-Hetem, J., & Casanova, S. 1998, *MNRAS*, 300, 733
- Martín, E. L., Rebolo, R., & Zapatero Osorio, M. R. 1996, *ApJ*, 469, 706
- Martini, P., Stoll, R., Derwent, M. A., et al. 2011, *PASP*, 123, 187
- McClure, M. K., Furlan, E., Manoj, P., et al. 2010, *ApJS*, 188, 75
- Merin, B. Brown, J. M., Oliveira, I., et al. 2010, *ApJ*, 718, 1200
- Montmerle, T., Kock-Miramon, L., Falgarone, E., & Grindlay, J. E. 1983, *ApJ*, 269, 182
- Muzić, K., Scholz, A., Geers, V., Jayawardhana, R., & Tamura, M. 2012, *ApJ*, 744, 134
- Natta, A., Testi, L., Comeron, F., et al. 2002, *A&A*, 393, 597
- Natta, A., Testi, L., & Randich, S. 2006, *A&A*, 452, 245
- Ortiz-León, G. N., Loinard, L., Dzib, S. A., et al. 2018, *ApJ*, 869, L33
- Ortiz-León, G. N., Loinard, L., Kounkel, M. A. et al. 2017, *ApJ*, 834, 141
- Ozawa, H., Grosso, N., & Montmerle, T. 2005, *A&A*, 438, 661
- Patterer, R. J., Lawrence, R., Welty, A. D., & Huenemoerder, D. P. 1993, *AJ*, 105, 1519
- Pecaut, M. J. & Mamajek, E. E. 2016, *MNRAS*, 461, 794
- Pecaut, M. J., Mamajek, E. E., & Bubar, E. J. 2012, *ApJ*, 746, 154
- Perryman, M. A. C., de Boer, K. S., Gilmore, G., et al. 2001, *A&A*, 369, 339
- Pillitteri, I., Wolk, S. J., Chen, H. H., & Goodman A. 2016, *A&A*, 592, A88
- Prato, L. 2007, *ApJ*, 657, 338
- Prato, L., Greene, T. P., & Simon, M. 2003, *ApJ*, 584, 853
- Preibisch, T., Guenther, E., Zinnecker, H., et al. 1998, *A&A*, 333, 619
- Rayner, J. T., Cushing, M. C., & Vacca, W. D. 2009, *ApJS*, 185, 289
- Rayner, J. T., Toomey, D. W., Onaka, P. M., et al. 2003, *PASP*, 115, 362
- Riaz, B., Gizis, J. E., & Harvin, J. 2006, *AJ*, 132, 866
- Ridge, N. A., Di Francesco, J., Kirk, H., et al. 2006, *AJ*, 131, 2921
- Rieke, G. H., Su, K. Y. L., Stansberry, J. A., et al. 2005, *ApJ*, 620, 1010
- Rieke, G. H., Young, E. T., Engelbracht, C. W., et al. 2004, *ApJS*, 154, 25
- Rigliaco, E., Wilking, B., Meyer, M. R., et al. 2016, *A&A*, 588, A123
- Rizzuto, A. C., Ireland M. J., & Kraus, A. L. 2015, *MNRAS*, 448, 2737
- Romero, G. A., Schreiber, M. R., Cieza, L. A., et al. 2012, *ApJ*, 749, 79
- Rydgren, A. E. 1980, *AJ*, 85, 438
- Seale, J. P. & Looney, L. W. 2008, 675, 427
- Schlafly, E. F., Meisner, A. M., Stutz, A. M., et al. 2016, *ApJ*, 821, 78
- Skrutskie, M., Cutri, R. M., Stiening, R., et al. 2006, *AJ*, 131, 1163
- Slesnick, C. L., Carpenter, J. M., & Hillenbrand, L. A. 2006, *AJ*, 131, 3016
- Slesnick, C. L., Hillenbrand, L. A., & Carpenter, J. M. 2008, *ApJ*, 688, 377
- Stauffer, J., Rebull, L. David, T. J., et al. 2018, *AJ*, 155, 63
- Struve, O. & Rudkjøbing M. 1949, *ApJ*, 109, 92
- Testi, L., Natta, A., Oliva E., et al. 2002, *ApJ*, 571, 155
- Torres, C. A. O., Quast, G. R., Da Silva, L., et al. 2006, *A&A*, 460, 695
- Vacca, W. D., Cushing, M. C., & Rayner, J. T. 2003, *PASP*, 115, 389
- Vrba, F. J., Coyne, G. V., & Tapia, S. 1993, *AJ*, 105, 1010
- Vrba, F. J., Strom, K. M., Strom, S. E., & Grasdalen, G. L. 1975, *ApJ*, 197, 77
- Walter, F. M., Vrba, F. J., Mathieu, R. D., Brown, A. & Myers, P. C. 1994, *AJ*, 107, 692
- Werner, M. W., Roellig, T. L., Low, F. J., et al. 2004, *ApJS*, 154, 1
- Whelan, E. T., Riaz, B., & Rouze, B. 2018, *A&A*, 610, 19
- Wilking, B. A., Gagnè, M., & Allen, L. E. 2008, in *ASP Monograph Ser. 5, Handbook of Star-forming Regions, The Southern Sky, Vol. 2* ed. B. Reipurth (ASP: San Francisco, CA), 351
- Wilking, B. A., Greene, T. P., & Meyer, M. R. 1999, *AJ*, 117, 469
- Wilking, B. A. & Lada, C. J. 1983, *ApJ*, 274, 698
- Wilking, B. A., Lada, C. J., & Young, E. T. 1989, *ApJ*, 340, 823
- Wilking, B. A., Meyer, M. R., Robinson, J. G., & Greene, T. P. 2005, *AJ*, 130, 1733
- Wilking, B. A., Schwartz, R. D., & Blackwell, J. H. *AJ*, 94, 106
- Wilson, J. C., Skrutskie, M. F., Colonna, M. R., et al. 2001, *PASP*, 113, 227
- Wright, E. L., Eisenhardt, P. R., Mainzer, A. K., et al. 2010, *AJ*, 140, 1868



TABLE 1  
MEMBERS OF THE OPHIUCHUS COMPLEX

Column Label	Description
2MASS	2MASS Point Source Catalog source name
UGCS	UKIDSS Galactic Clusters Survey source name <sup>a</sup>
WISE	WISE source name <sup>b</sup>
Gaia	Gaia DR2 source name
SR	Designation from Struve & Rudkjøbing (1949)
DoAr	Designation from Dolidze & Arakelian (1959)
GSS	Designation from Grasdalen et al. (1973)
VSSG	Designation from Vrba et al. (1975)
Elias	Designation from Elias (1978)
ROX	Designation from Montmerle et al. (1983)
WL	Designation from Wilking & Lada (1983)
WSB	Designation from Wilking et al. (1987)
HBC	Designation from Herbig & Bell (1988)
WLY	Designation from Wilking et al. (1989)
LFAM	Designation from Leous et al. (1991)
GY	Designation from Greene & Young (1992)
ROXs	Designation from Bouvier & Appenzeller (1992)
ROXR1	Designation from Casanova et al. (1995)
ROXA	Designation from Kamata et al. (1997)
RXJ	Designation from Martín et al. (1998)
ROXR	Designation from Grosso et al. (2000)
ISO-Oph	Designation from Bontemps et al. (2001)
ROXN	Designation from Ozawa et al. (2005)
CFHTWIR-Oph	Designation from Alves de Oliveira et al. (2010)
OName	Other common identifier
RAdeg	Right Ascension (J2000)
DEdeg	Declination (J2000)
Ref-Pos	Reference for RAdeg and DEdeg <sup>c</sup>
Region	Region in Figure 1
SpType	Spectral Type
r.SpType	Reference for SpType <sup>d</sup>
Adopt	Adopted spectral type
GaiapmRA	Proper motion in RA from <i>Gaia</i> DR2
e.GaiapmRA	Error in GaiapmRA
GaiapmDec	Proper motion in DE from <i>Gaia</i> DR2
e.GaiapmDec	Error in GaiapmDec
plx	Parallax from <i>Gaia</i> DR2
e.plx	Error in plx
Gmag	$G$ magnitude from <i>Gaia</i> DR2
e.Gmag	Error in Gmag
GBPmag	$G_{BP}$ magnitude from <i>Gaia</i> DR2
e.GBPmag	Error in GBPmag
GRPmag	$G_{RP}$ magnitude from <i>Gaia</i> DR2
e.GRPmag	Error in GRPmag
RUWE	Re-normalized unit weight error from Lindegren (2018)
IRpmRA	Proper motion in RA from IRAC
e.IRpmRA	Error in IRpmRA
IRpmDec	Proper motion in DE from IRAC
e.IRpmDec	Error in IRpmDec
Jmag	$J$ magnitude
e.Jmag	Error in Jmag
r.Jmag	Reference for Jmag <sup>e</sup>
Hmag	$H$ magnitude
e.Hmag	Error in Hmag
r.Hmag	Reference for Hmag <sup>e</sup>
Kmag	$K_s$ or $K$ magnitude
e.Kmag	Error in Kmag
r.Kmag	Reference for Kmag <sup>e</sup>
3.6mag	<i>Spitzer</i> [3.6] magnitude
e.3.6mag	Error in 3.6mag
f.3.6mag	Flag on 3.6mag <sup>f</sup>
4.5mag	<i>Spitzer</i> [4.5] magnitude
e.4.5mag	Error in [4.5] magnitude
f.4.5mag	Flag on 4.5mag <sup>f</sup>
5.8mag	<i>Spitzer</i> [5.8] magnitude
e.5.8mag	Error in 4.5mag
f.5.8mag	Flag on 5.8mag <sup>f</sup>
8.0mag	<i>Spitzer</i> [8.0] magnitude
e.8.0mag	Error in 8.0mag
f.8.0mag	Flag on 8.0mag <sup>f</sup>
24mag	<i>Spitzer</i> [24] magnitude
e.24mag	Error in 24mag
f.24mag	Flag on 24mag <sup>f</sup>
W1mag	<i>WISE</i> W1 magnitude

TABLE 1 — *Continued*

Column Label	Description
e.W1mag	Error in W1mag
f.W1mag	Flag on W1mag <sup>f</sup>
W2mag	<i>WISE</i> W2 magnitude
e.W2mag	Error in W2mag
f.W2mag	Flag on W2mag <sup>f</sup>
W3mag	<i>WISE</i> W3 magnitude
e.W3mag	Error in W3mag
f.W3mag	Flag on W3mag <sup>f</sup>
W4mag	<i>WISE</i> W4 magnitude
e.W4mag	Error in W4mag
f.W4mag	Flag on W4mag <sup>f</sup>
Exc4.5	Excess present in [4.5]?
Exc8.0	Excess present in [8.0]?
Exc24	Excess present in [24]?
ExcW2	Excess present in <i>W</i> 2?
ExcW3	Excess present in <i>W</i> 3?
ExcW4	Excess present in <i>W</i> 4?
DiskType	Disk Type
Ak	Extinction in K
f.Ak	Method for estimating Ak <sup>g</sup>

NOTE. — This table is available in its entirety in a machine-readable form.

<sup>a</sup> Based on coordinates from Data Release 10 of the UKIDSS Galactic Clusters Survey for stars with  $K_s > 10$  from 2MASS.

<sup>b</sup> Coordinate-based identifications from the AllWISE Source Catalog when available. Otherwise, identifications are from the AllWISE Reject Table or the WISE All-Sky Catalog.

<sup>c</sup> 2MASS = 2MASS Point Source Catalog; UKIDSS = UKIDSS DR10 Catalog; Gaia = Gaia DR2; Kraus14 = Kraus et al. (2014).

<sup>d</sup> 1 = Luhman & Esplin (2020); 2 = Luhman et al. (2018); 3 = Martín et al. (1998); 4 = Prato (2007); 5 = This work; 6 = Romero et al. (2012); 7 = McClure et al. (2010); 8 = Esplin et al. (2018); 9 = Gully-Santiago et al. (2012); 10 = Allers et al. (2007); 11 = Preibisch et al. (1998); 12 = Riaz et al. (2006); 13 = Cieza et al. (2010); 14 = Merin et al. (2010); 15 = Slesnick et al. (2006); 16 = Rizzuto et al. (2015); 17 = Erickson et al. (2011); 18 = Wilking et al. (2005); 19 = Prato et al. (2003); 20 = Cohen & Kuhl (1979); 21 = Maheswar et al. (2003); 22 = Alves de Oliveira et al. (2012); 23 = Houk & Smith-Moore (1998); 24 = Greene & Meyer (1995); 25 = Luhman & Rieke (1999); 26 = Bouvier & Appenzeller (1992); 27 = Pecaut & Mamajek (2016); 28 = Alves de Oliveira et al. (2010); 29 = Walter et al. (1994); 30 = Stauffer et al. (2018); 31 = Struve & Rudkjøbing (1949); 32 = Mužić et al. (2012); 33 = Slesnick et al. (2008); 34 = Ansdell et al. (2016); 35 = Wilking et al. (1999); 36 = Natta et al. (2002); 37 = Manara et al. (2015); 38 = Cody et al. (2017); 39 = Testi et al. (2002); 40 = Comerón et al. (2010); 41 = Cushing et al. (2000); 42 = Luhman et al. (1997); 43 = Herczeg & Hillenbrand (2014); 44 = Gatti et al. (2006); 45 = Geers et al. (2007); 46 = Natta et al. (2006); 47 = Rydgren (1980); 48 = Bowler et al. (2014); 49 = Torres et al. (2006); 50 = Vrba et al. (1993); 51 = Whelan et al. (2018).

<sup>e</sup> 2MASS = 2MASS Point Source Catalog; UKIDSS = UKIDSS Data Release 10; ISPI = our ISPI photometry (Sec 3.3); VHS = VHS Data Release 6.

<sup>f</sup> nodet = non-detection; sat = saturated; out = outside of the camera's field of view; bl = photometry may be affected by blending with a nearby star; bin = includes an unresolved binary companion; err = W2 magnitudes brighter than 6 mag are erroneous; unres = too close to a brighter star to be detected; ext = photometry is known or suspected to be contaminated by extended emission (no data given when extended emission dominates); false = detection from WISE catalog appears false or unreliable based on visual inspection.

<sup>g</sup> J-H and H-K = derived from these colors assuming photospheric near-IR colors (Luhman & Esplin 2020); IR spec = derived from an IR spectrum.

TABLE 2  
YOUNG NON-MEMBERS TOWARD THE OPHIUCHUS COMPLEX

Column Label	Description
2MASS	2MASS Point Source Catalog source name
UGCS	UKIDSS Galactic Clusters Survey source name <sup>a</sup>
WISE	WISE source name <sup>b</sup>
Gaia	Gaia DR2 source name
SR	Designation from Struve & Rudkjøbing (1949)
DoAr	Designation from Dolidze & Arakelian (1959)
GSS	Designation from Grasdalen et al. (1973)
VSSG	Designation from Vrba et al. (1975)
Elias	Designation from Elias (1978)
ROX	Designation from Montmerle et al. (1983)
WSB	Designation from Wilking et al. (1987)
HBC	Designation from Herbig & Bell (1988)
WLY	Designation from Wilking et al. (1989)
LFAM	Designation from Leous et al. (1991)
GY	Designation from Greene & Young (1992)
ROXs	Designation from Bouvier & Appenzeller (1992)
ROXR1	Designation from Casanova et al. (1995)
ROXA	Designation from Kamata et al. (1997)
RXJ	Designation from Martín et al. (1998)
ROXR	Designation from Grosso et al. (2000)
ISO-Oph	Designation from Bontemps et al. (2001)
OName	Other common identifier
RAdeg	Right Ascension (J2000) from Gaia DR2
DEdeg	Declination (J2000) from Gaia DR2
SpType	Spectral Type
r_SpType	Reference for SpType <sup>c</sup>
Adopt	Adopted spectral type
GaiapmRA	Proper motion in RA from <i>Gaia</i> DR2
e_GaiapmRA	Error in GaiapmRA
GaiapmDec	Proper motion in DE from <i>Gaia</i> DR2
e_GaiapmDec	Error in GaiapmDec
plx	Parallax from <i>Gaia</i> DR2
e_plx	Error in plx
Gmag	$G$ magnitude from <i>Gaia</i> DR2
e_Gmag	Error in Gmag
GBPmag	$G_{BP}$ magnitude from <i>Gaia</i> DR2
e_GBPmag	Error in GBPmag
GRPmag	$G_{RP}$ magnitude from <i>Gaia</i> DR2
e_GRPmag	Error in GRPmag
RUWE	Re-normalized unit weight error from Lindegren (2018)
Jmag	$J$ magnitude from the 2MASS Point Source Catalog
e_Jmag	Error in Jmag
Hmag	$H$ magnitude from the 2MASS Point Source Catalog
e_Hmag	Error in Hmag
Kmag	$K_s$ magnitude from the 2MASS Point Source Catalog
e_Kmag	Error in Kmag
Pops	Gaia parallax and proper motion consistent with these populations <sup>d</sup>

NOTE. — This table is available in its entirety in a machine-readable form.

<sup>a</sup> Based on coordinates from Data Release 10 of the UKIDSS Galactic Clusters Survey for stars with  $K_s > 10$  from 2MASS.

<sup>b</sup> Coordinate-based identifications from the AllWISE Source Catalog when available. Otherwise, identifications are from the AllWISE Reject Table or the WISE All-Sky Catalog.

<sup>c</sup> 1 = Martín et al. (1998); 2 = Gully-Santiago et al. (2012); 3 = This work; 4 = Houk & Smith-Moore (1998); 5 = Esplin et al. (2018); 6 = Walter et al. (1994); 7 = Garrison (1967); 8 = Hernández et al. (2005); 9 = Wilking et al. (2005); 10 = Erickson et al. (2011); 11 = Bouvier & Appenzeller (1992); 12 = Luhman & Rieke (1999); 13 = Herczeg & Hillenbrand (2014); 14 = Rizzuto et al. (2015); 15 = Wilking et al. (1999); 16 = Mužić et al. (2012); 17 = Cohen & Kuhl (1979); 18 = Greene & Meyer (1995); 19 = Torres et al. (2006); 20 = Slesnick et al. (2008); 21 = Pecaut & Mamajek (2016); 22 = Patterer et al. (1993); 23 = Vrba et al. (1993); 24 = McClure et al. (2010); 25 = Cieza et al. (2010).

<sup>d</sup> O/o = Ophiuchus; U/u = Upper Sco; S/s = remainder of Sco-Cen; n = none of those populations. Upper case letters indicate that both proper motion and parallax support membership in that population. Lower case letters indicate that either proper motion or parallax supports membership while the other parameter is inaccurate, unreliable, or unavailable.

TABLE 3  
IRAC OBSERVATIONS OF OPHIUCHUS

AOR	PID	PI	epoch
3651840	6	G. Fazio	2004.2
3652096	6	G. Fazio	2004.2
3660800	6	G. Fazio	2004.2
3661056	6	G. Fazio	2004.2
5672192	173	N. Evans	2004.6

NOTE. — This table is available in its entirety in machine-readable form. A portion is shown is here for guidance regarding its form and content.

TABLE 4  
CANDIDATE MEMBERS OF UPPER SCO AND OPHIUCHUS

Column Label	Description
2MASS	2MASS Point Source Catalog source name
WISEA	ALLWISE Source Catalog source name
UGCS	UKIDSS Galactic Clusters Survey source name <sup>a</sup>
Gaia	<i>Gaia</i> DR2 source name
RAdeg	Right Ascension (J2000)
DEdeg	Declination (J2000)
Ref-Pos	Reference for RAdeg and DEdeg <sup>b</sup>
pmRA	Proper motion in right ascension from <i>Gaia</i> DR2
e_pmRA	Error in pmRA
pmDec	Proper motion in declination from <i>Gaia</i> DR2
e_pmDec	Error in pmDec
plx	Parallax from <i>Gaia</i> DR2
e_plx	Error in plx
Gmag	<i>G</i> magnitude from <i>Gaia</i> DR2
e_Gmag	Error in Gmag
GBPmag	<i>G</i> <sub>BP</sub> magnitude from <i>Gaia</i> DR2
e_GBPmag	Error in GBPmag
GRPmag	<i>G</i> <sub>RP</sub> magnitude from <i>Gaia</i> DR2
e_GRPmag	Error in GRPmag
RUWE	renormalized unit weight error from Lindegren (2018)
Jmag	<i>J</i> magnitude
e_Jmag	Error in Jmag
r_Jmag	Reference for Jmag <sup>c</sup>
Hmag	<i>H</i> magnitude
e_Hmag	Error in Hmag
r_Hmag	Reference for Hmag <sup>c</sup>
Kmag	<i>K</i> <sub>s</sub> magnitude
e_Kmag	Error in Kmag
r_Kmag	Reference for Kmag <sup>c</sup>
selection	Selection criteria satisfied by candidate <sup>d</sup>
separation	Angular separation from nearest known young star within 5''
compGaia	<i>Gaia</i> DR2 source name of nearest known young star within 5''

NOTE. — The table is available in its entirety in machine-readable form.

<sup>a</sup> Based on coordinates from DR10 of the UKIDSS Galactic Clusters Survey for stars with  $K_s > 10$  from 2MASS.

<sup>b</sup> Sources of the right ascension and declination are DR2 of *Gaia*, DR10 of the UKIDSS Galactic Clusters Survey, and the 2MASS Point Source Catalog.

<sup>c</sup> 2MASS = 2MASS Point Source Catalog; UKIDSS = UKIDSS Data Release 10; ISPI = our ISPI photometry (Sec 3.3); VHS = VHS Data Release 6.

<sup>d</sup>  $G/ip/zp/yp/Z/Y/H/[3.6]/[4.5]$  = CMDs from Figure 5; pi = parallax/proper motions from *Gaia* DR2; irac = proper motions from IRAC.

TABLE 5  
OBSERVING LOG

Telescope/Instrument	Disperser/Aperture	Wavelengths/Resolution	Targets
IRTF/Spex	prism/0''8 slit	0.8–2.5 $\mu\text{m}/R = 150$	96
Gemini North/GNIRS	31.7 l mm <sup>-1</sup> /1'' slit	0.9–2.5 $\mu\text{m}/R = 600$	7
4m Blanco CTIO/COSMOS	red VPH/0''9 slit	0.55–0.95 $\mu\text{m}/3 \text{ \AA}$	41
4m Blanco CTIO/ARCoIRIS	110.5 l mm <sup>-1</sup> + prism/1''1 slit	0.8–2.47 $\mu\text{m}/3500$	56
Gemini South/FLAMINGOS-2	HK Grism/0''72 slit	1.10–2.65 $\mu\text{m}/450$	4
Magellan/CorMASS	40 l mm <sup>-1</sup> + prism/0''4 slit	0.8–2.5 $\mu\text{m}/300$	24
Magellan/IMACS	200 l mm <sup>-1</sup> grism/0''9 slit	0.5–1.0 $\mu\text{m}/7 \text{ \AA}$	4

TABLE 6  
SPECTROSCOPIC DATA FOR CANDIDATE MEMBERS OF OPHIUCHUS AND UPPER  
SCO

Source Name <sup>a</sup>	Spectral Type	Instrument	Date	Young?	Adopted Member of Oph?
2MASS J16200698-2430501	M5	SpeX	2016 Apr 8	Y	N
2MASS J16201835-2409537	M3.5	SpeX	2016 Apr 7	Y	N
2MASS J16202629-2416226	M3.5	ARCoIRIS	2016 Jun 19	Y	N
2MASS J16204233-2431473	M3	ARCoIRIS	2016 Jun 18	Y	N
2MASS J16204607-2430599	M2.5	ARCoIRIS	2016 Jun 18	Y	N

NOTE. — This table is available in its entirety in a machine-readable form. A portion is shown is here for guidance regarding its form and content.

<sup>a</sup> Identifications from the 2MASS Point Source Catalog when available. Otherwise, they based on coordinates from data release 10 of the UKIDSS Galactic Clusters Survey.

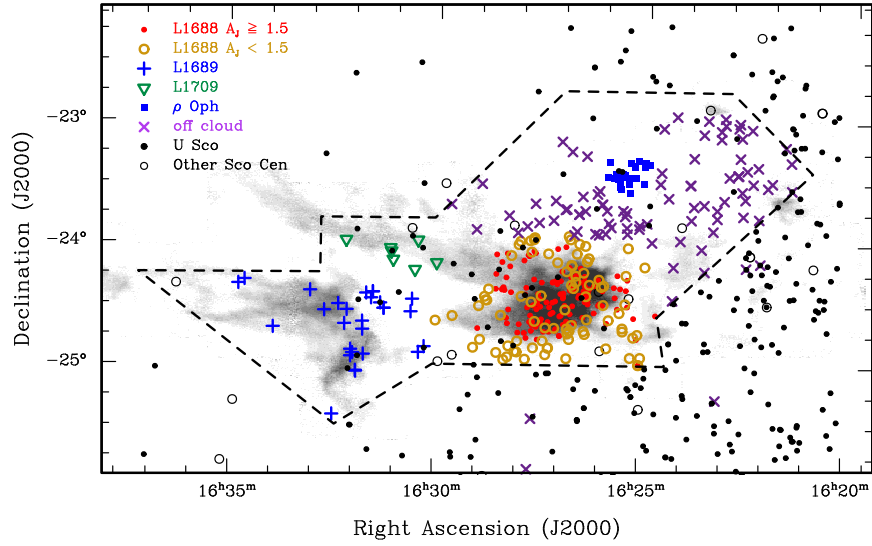


FIG. 1.— Spatial distribution of known young stars in the vicinity of the Ophiuchus complex. Our adopted members of Ophiuchus (Table 1) are assigned symbols based on positions toward L1688 (red filled circles and yellow open circles), L1689 (blue plus signs), L1709 (green open triangles), the  $\rho$  Oph cluster (blue filled squares), and areas without dark clouds (purple crosses). Young stars that are not adopted Ophiuchus members consist of members of Upper Sco (black filled circles) and other populations in Sco-Cen (black open circles). The dashed line indicates the boundary between Ophiuchus and Upper Sco from Esplin et al. (2018). The dark clouds of Ophiuchus are represented by a map of  $^{13}\text{CO}$  emission (Ridge et al. 2006).

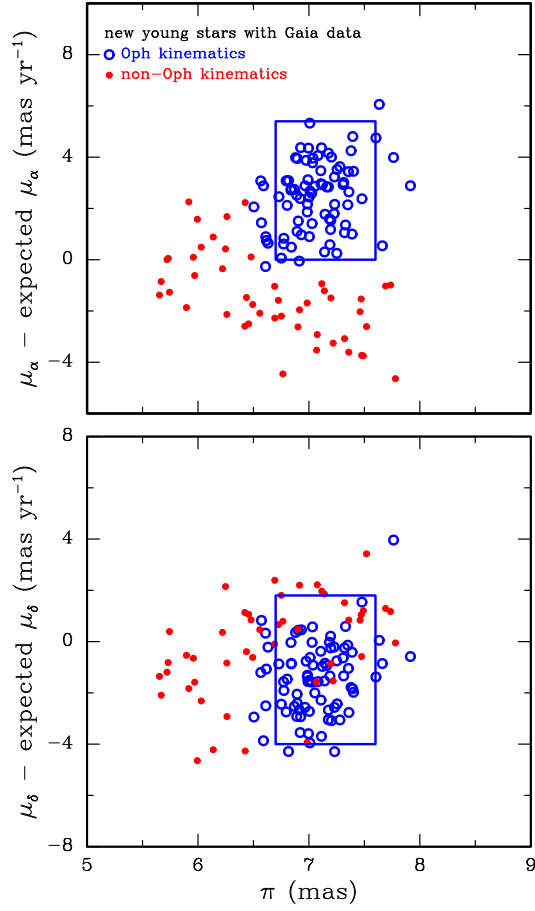


FIG. 2.— Proper motion offsets versus parallax for new young stars from our spectroscopic sample that have parallaxes and proper motions from *Gaia* DR2. We have indicated our adopted thresholds for membership in Ophiuchus (rectangles, Luhman & Esplin 2020). Stars with  $1\sigma$  errors that overlap with those thresholds are adopted as Ophiuchus members (blue open circles). The remaining stars have kinematics that are consistent with membership in Upper Sco or other populations in Sco-Cen (red closed circles). The stars have been assigned symbols based on whether they satisfy those criteria (at  $1\sigma$ ). The proper motion offsets are relative to the values expected for the positions and parallaxes of the stars assuming a space velocity of  $U = -5$ ,  $V = -16$ , and  $W = -7$  km s $^{-1}$ . Errors in parallax and proper motion offsets range from 0.03–0.7 mas and 0.06–1.63 mas/yr, respectively.

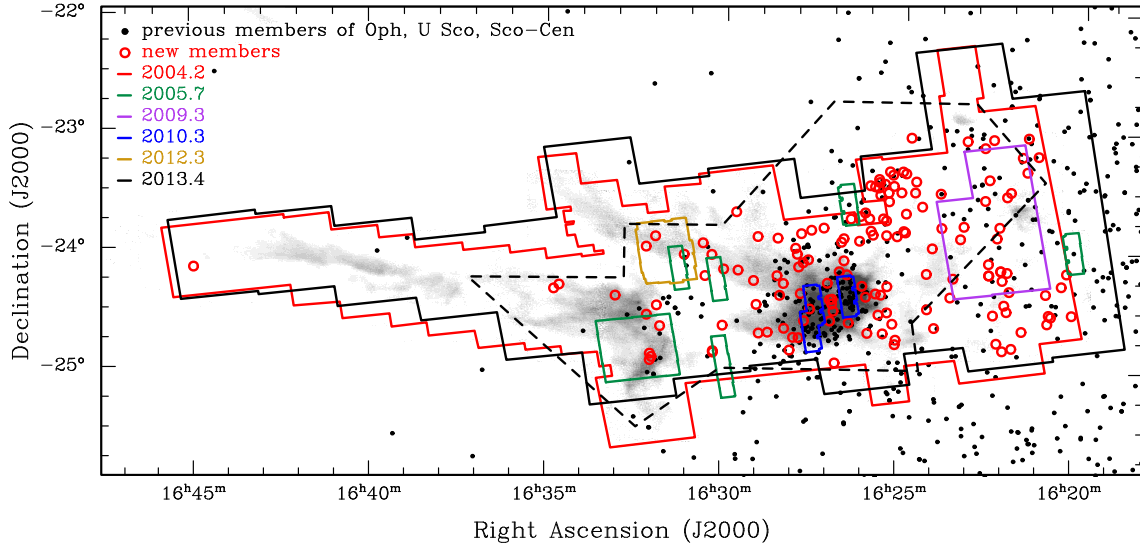


FIG. 3.— Map of the largest fields in Ophiuchus that were imaged by IRAC (Table 3), which span a wide range of epochs. We have included the previously known members of Ophiuchus, Upper Sco, and Sco Cen near the Ophiuchus dark clouds (black filled circles) and members discovered in this work (red open circles).



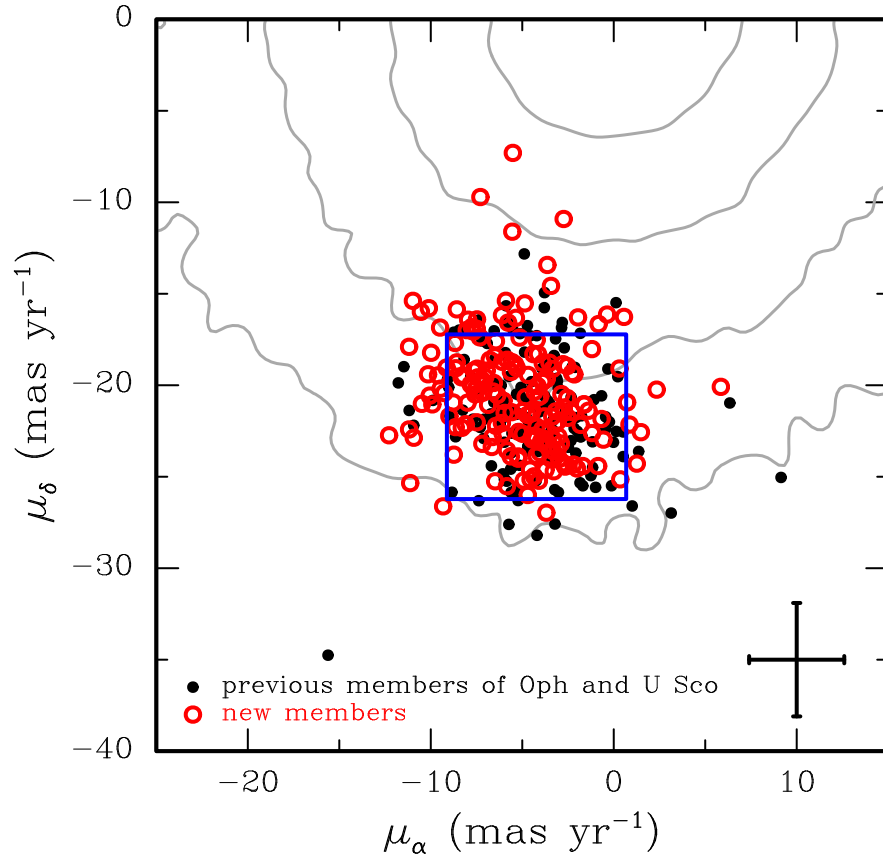


FIG. 4.— Relative proper motions measured from multi-epoch IRAC imaging for previously known members of Ophiuchus and Upper Sco (black filled circles) and new members discovered in this work (red open circles). Measurements for other sources in the IRAC images are represented by contours at  $\log(\text{numbers}/(\text{mas yr}^{-1})^2) = 1.0, 1.5, 2.0, \text{ and } 2.5$ . The typical errors are indicated (error bars).

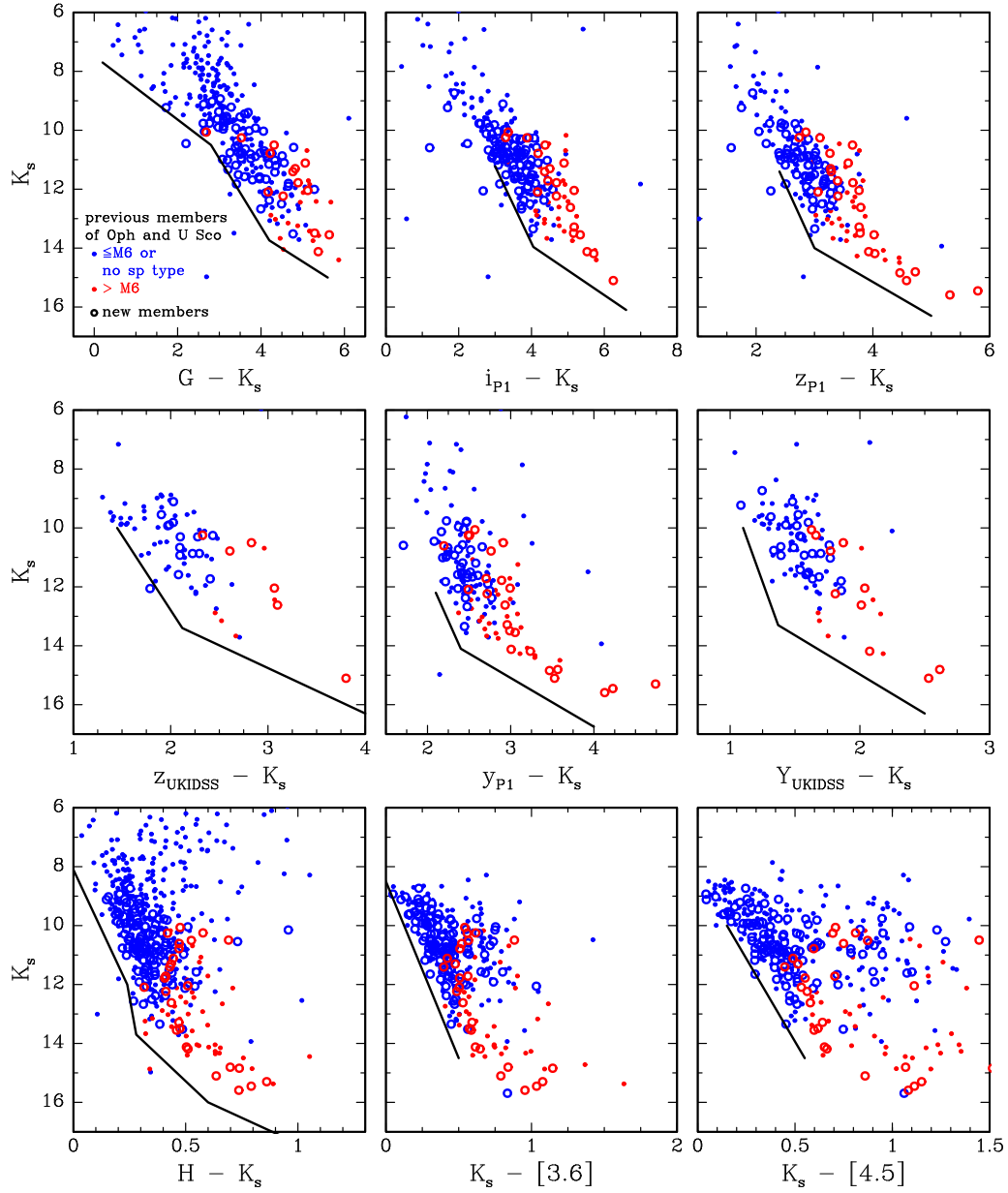


FIG. 5.— Extinction-corrected CMDs for previously known members of Ophiuchus and Upper Sco within Figure 3 (filled circles) and new members from this work (open circles). Candidate members were identified based on their positions above the solid boundaries.

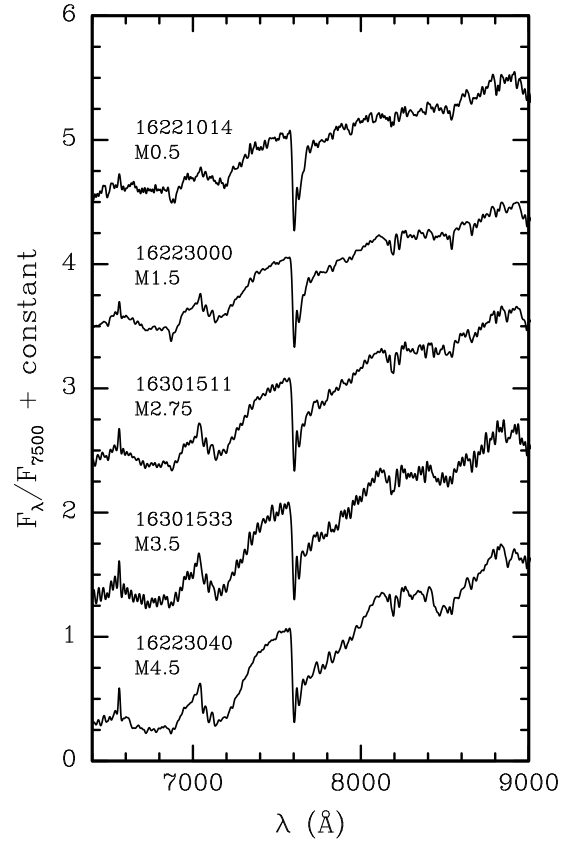


FIG. 6.— Examples of optical spectra of new members of Ophiuchus and Upper Sco (Table 6). These data are displayed at a resolution of 13  $\text{\AA}$ . The data used to create this figure are available.

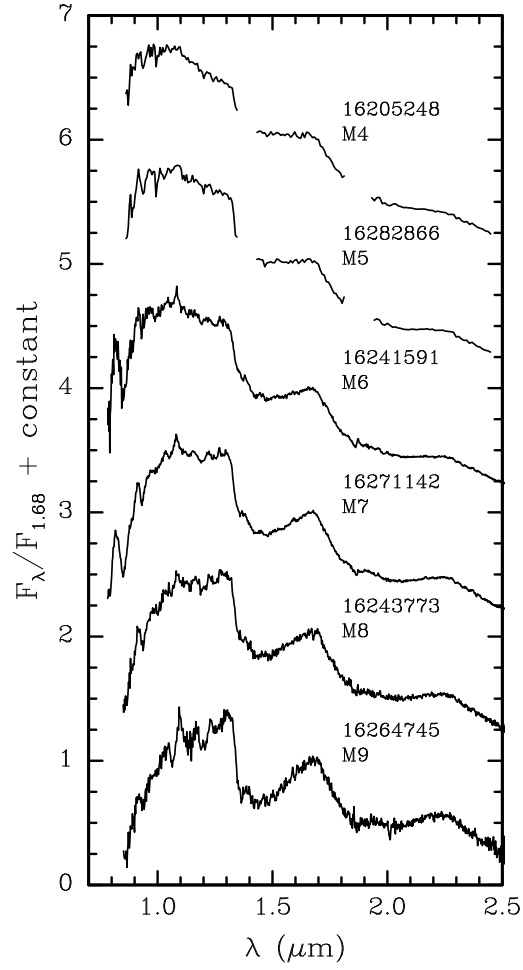


FIG. 7.— Examples of IR spectra of new members of Ophiuchus and Upper Sco (Table 6). The spectra have been dereddened to match the slopes of the young standards from Luhman et al. (2017). The data used to create this figure are available.

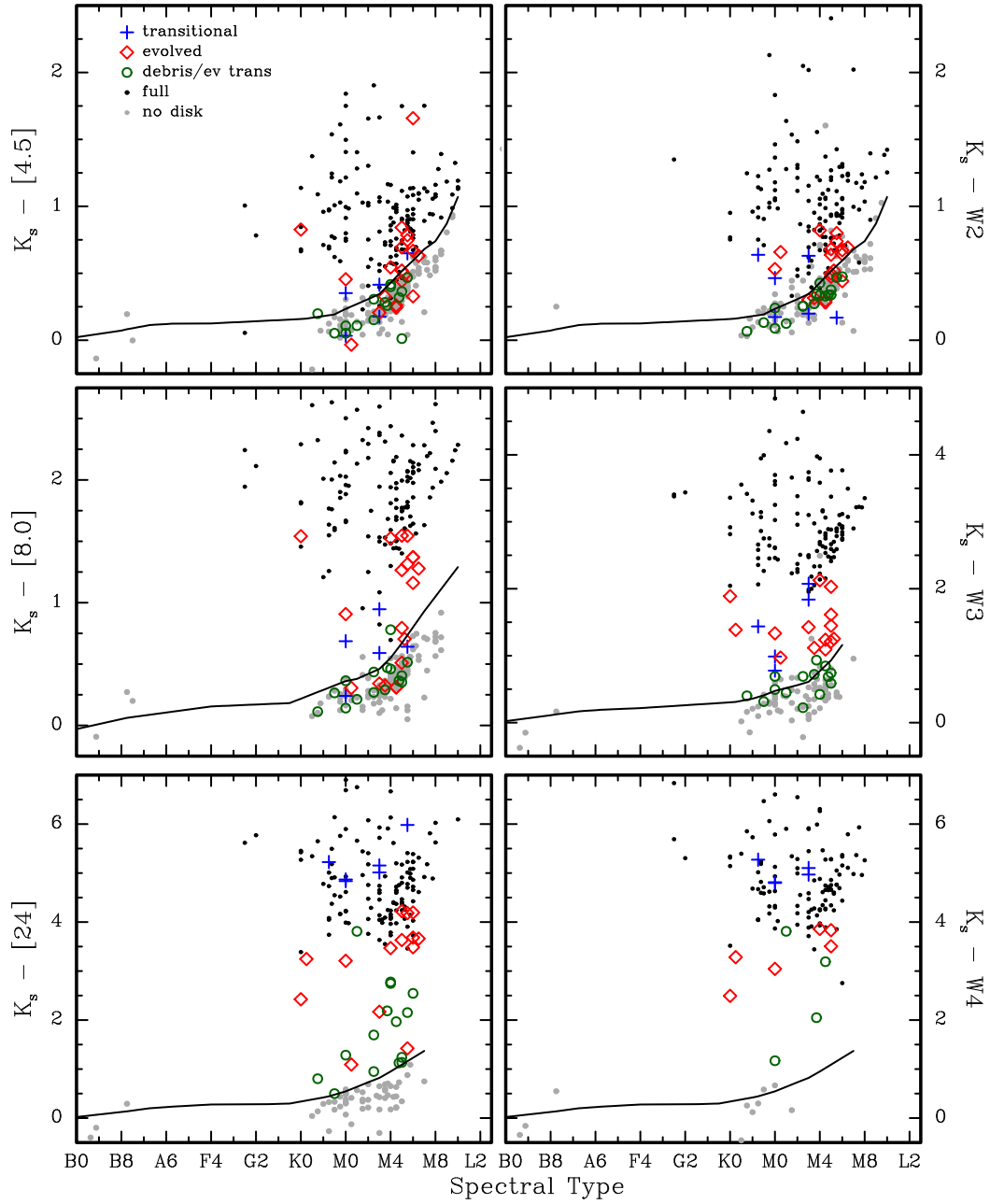


FIG. 8.— Extinction-corrected IR colors as a function of spectral type for known members of Ophiuchus. In each color, we have marked a boundary that has been used to identify the presence of color excess from circumstellar disks (solid lines), which were selected to follow the observed photospheric sequences (Esplin et al. 2018).

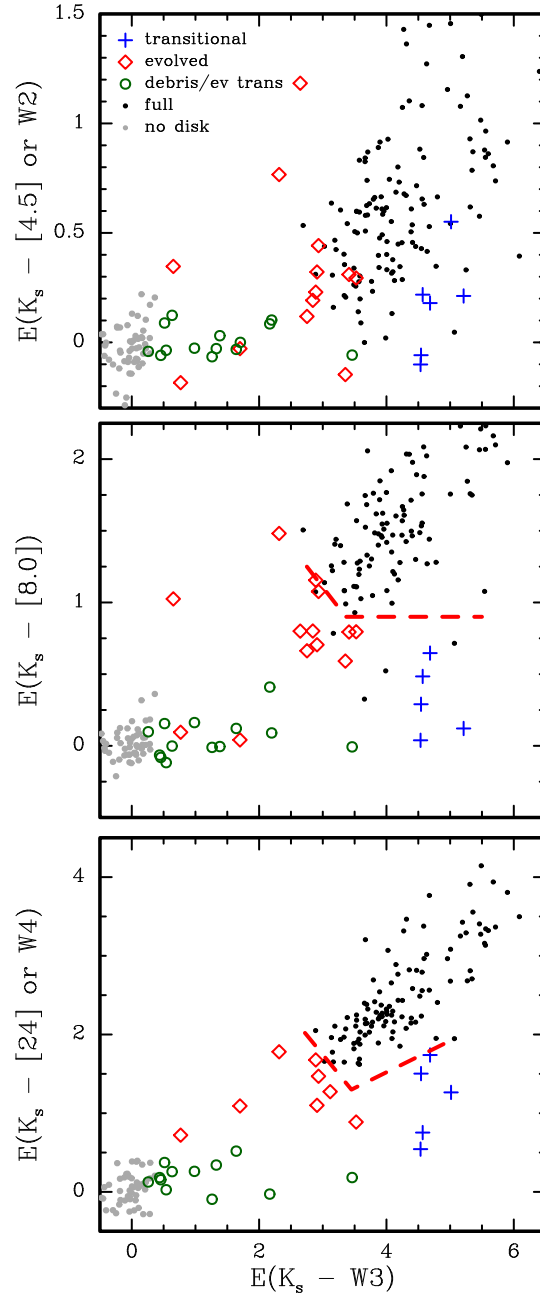


FIG. 9.— Extinction-corrected IR color excesses for known members of Ophiuchus. Data at [4.5] and [24] are shown when available. Otherwise, data from the similar bands of  $W2$  and  $W4$  are used. In the bottom two diagrams, we indicate the boundaries that are used to distinguish full disks from disks in more advanced stages of evolution and are defined in Esplin et al. (2014).

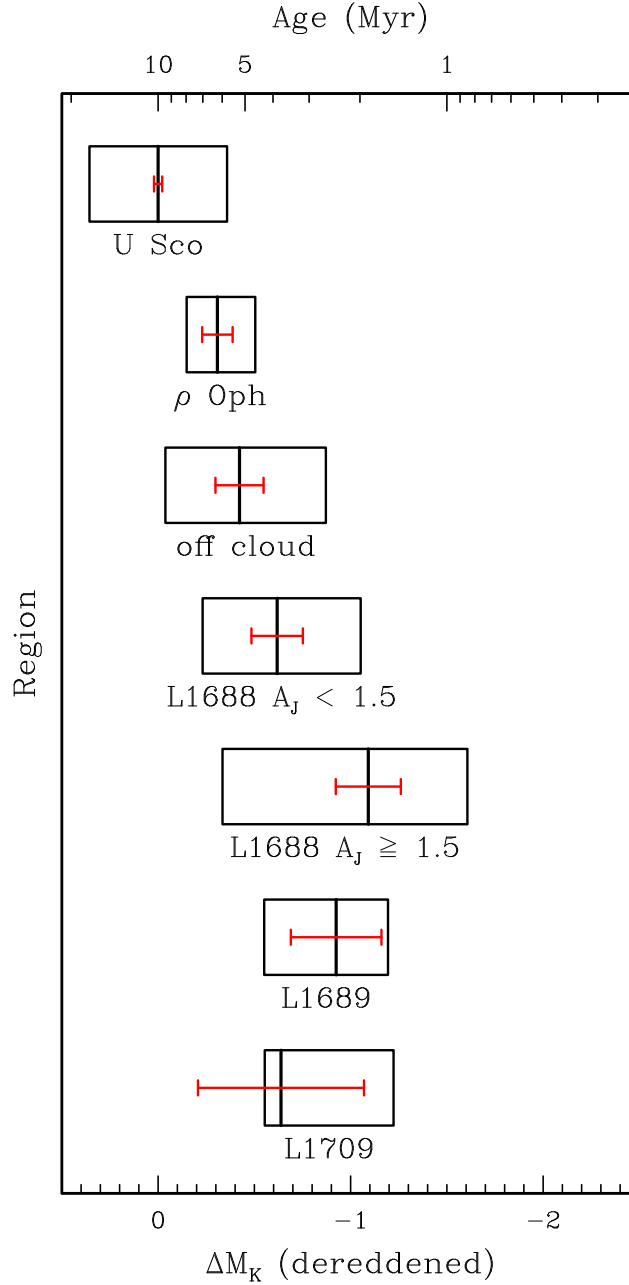


FIG. 10.— Box diagrams showing the medians (center vertical lines) and interquartile ranges (width of box) of the  $M_K$  offsets for the populations in Ophiuchus shown in Figure 1 and for known members of Upper Sco (Luhman & Esplin 2020). Offsets for the K5–M5 members are measured relative to the median  $M_K$  as a function of spectral type for members of Upper Sco. Errors for the median values of  $\Delta M_K$  have been estimated by bootstrapping (error bars). Smaller values of  $\Delta M_K$  correspond to brighter photometry, and hence younger ages. The top axis indicates the ages that correspond to  $\Delta M_K$  assuming an age of 10 Myr for Upper Sco and the change in luminosity with age predicted by evolutionary models (Baraffe et al. 2015).